Russian Journal of General Chemistry, Vol. 72, No. 7, 2002, pp. 997–1006. Translated from Zhurnal Obshchei Khimii, Vol. 72, No. 7, 2002, pp. 1067–1076.

Nanostructure of Dispersed and Compact Nonstoichiometric Vanadium Carbide

A. I. Gusev, A. A. Tulin, V. N. Lipatnikov, and A. A. Rempel'

Institute of Chemistry of Solids, Ural Division, Russian Academy of Sciences, Yekaterinburg, Russia

Received October 9, 2001

Abstract—Structure and properties of dispersed and compact nanocrystalline vanadium carbide $VC_{0.875}$ were studied. Dispersed vanadium nanocarbide was prepared by prolonged aging of a coarse-grained $VC_{0.875}$ powder. It has a unique nanostructure: nanocrystallites of dispersed vanadium carbide have a shape of bent lobes up to 600 nm in diameter and 15–20 nm thick. Annealing and quenching of compact samples of coarse-grained $VC_{0.875}$ carbide result in the formation of a nanodomain structure. The nanostructured carbide $VC_{0.875}$ corresponds in composition to the higher boundary of a homogeneity area of a cubic phase and mainly contains ordered V_8C_7 phase, which belongs to the $P4_332$ space group. Cold pressing and subsequent vacuum sintering of vanadium carbide nanopowder at 2000 K gave sintered samples approaching diamond in microhardness.

Nanocrystalline ceramic materials are being extensively studied today [1–5] with the aim to develop hard but non-brittle materials. Nonstoichiometric carbides of transition metals of Groups IV and V are promising in this respect, as they are inferior in hardness only to diamond and cubic boron nitride [6].

Transition metal carbides MC_y ($MC_y\square_{1-y}$) fall in the group of strongly nonstoichiometric compounds [7, 8]. The carbides $MC_y\square_{1-y}$ in the disordered state have a *B*1 cubic structure and can contain up to 50% of structural vacancies $\square$ in the nonmetal sublattice [7–10]. At $T < 1300$ K, the *B*1 structure becomes unstable, and disorder–order phase transitions take place in nonstoichiometric carbides to give ordered phases with complex superstructures [7–13]. Order–disorder transitions in carbides are the first-kind transitions [7–13] accompanied by jumpwise changes of volume. However, the ordering is a diffuse process and hence it occurs not instantaneously, but within a relatively long time. The carbides are synthesized at 1400–1800 K, i.e., at temperatures higher than the temperature of disorder–order phase transitions T_{trans}. On cooling from the synthesis temperature to room temperature, the nonstoichiometric carbide passes through the ordering temperature T_{trans} and tends to order. If the cooling is fast, the ordering has no time to be completed, and the nonstoichiometric carbide remains in the metastable disordered state. Owing to a difference in the lattice parameters of the disordered and ordered phases, stresses arise in a sample, which with time result in cracking of crystallites along the boundaries between the disordered and ordered phases. By controlling the domain size in the ordered phase, it is possible to obtain nanostructured nonstoichiometric carbides in dispersed and compact states.

Here we report on the structure and properties of nanocrystalline vanadium carbide. The nanostructured state was formed by a fundamentally new method: ordering of nonstoichiometric vanadium carbide. So far, the ordering phenomenon was not used for creating a nanostructure in a solid. The choice of vanadium carbide was governed by the fact that ordering in it is manifested most clearly [14–17]. Not only volume (related to particle sizes), but also surface (related to the state and structure of interfaces) effects in nanocrystalline solids and nanopowders are important [1–3]; therefore, in studying physicochemical properties of vanadium carbide, special attention was given to the state of its surface.

STRUCTURE AND COMPOSITION

Dispersed carbide. The initial $VC_{0.875}$ powder with a particle size of 1–2 μm was prepared by carbothermal reduction of V_2O_5 and then was subjected to prolonged aging at ambient temperature in a closed vessel without access of atmospheric moisture. Aged powder of vanadium carbide appeared to be highly hygroscopic: we found that, immediately after withdrawal from the vessel, the powder contained no more than 0.2 wt % physically adsorbed water, whereas after storage in air for several months the water con-

1070-3632/02/7207-0997 $27.00

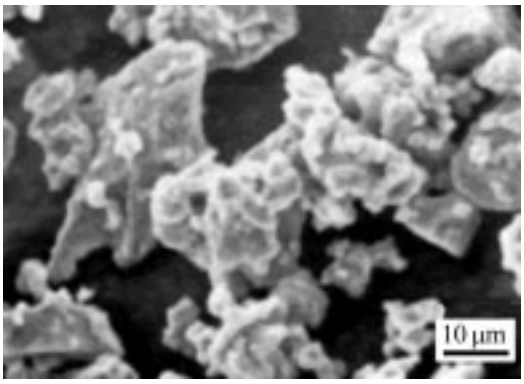

Fig. 1. Microstructure of an aged powder of vanadium carbide $VC_{0.875}$ at a 1000× magnification: irregular-shaped agglomerates of 5–50 μm size consist of ~1-μm particles.

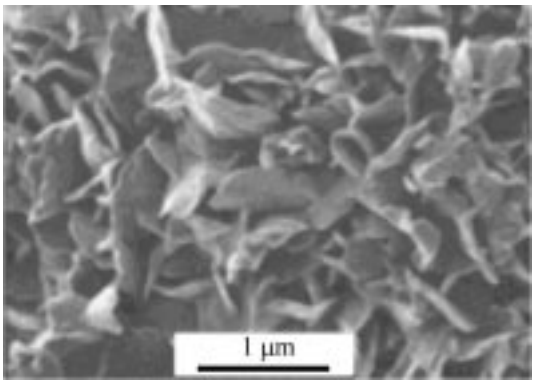

Fig. 2. Nanocrystallites of an aged powder of vanadium carbide $VC_{0.875}$ at a 20000× magnification.

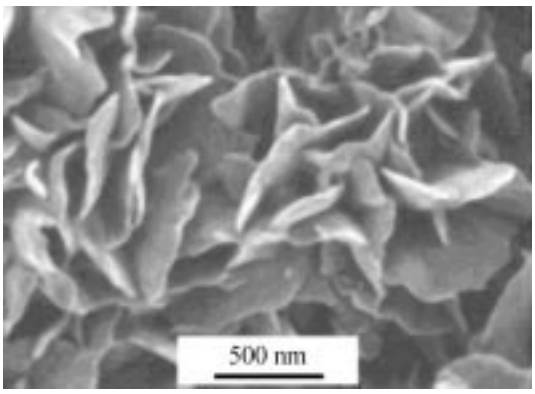

Fig. 3. Morphology of particles of an aged $VC_{0.875}$ powder at a 30000× magnification: particles about 1 μm in size consist of nanocrystallites with a shape of curved leaves (disks) with a diameter from 400 to 600 nm and a thickness of ~15–20 nm.

tent reached a saturation limit of 2.0 wt %. Common coarse-grained VC_y powder is considerably less hygroscopic; therefore, the high hygroscopicity of aged vanadium carbide powder is an indirect evidence of its highly developed surface.

According to chemical analysis, aged vanadium carbide has the composition $VC_{0.875}$ corresponding to the upper boundary of the homogeneity area of *B*1 cubic phase (NaCl). Impurities of Ti, Nb, and Ta (1 wt % in total) were detected by EDX analysis. The aged powder of vanadium carbide had the following elemental composition (wt %): V 76.8 ± 0.1; C_{bound} 15.9 ± 0.1; C_{free} 0.9 ± 0.1; H_2O 2.0 ± 0.2; O_{chem} 3.1 ± 0.1; O_{latt} 0.1; N 0.2 ± 0.02; and Ti, Nb, Ta 1.0 ± 0.1.

The total oxygen content (5.0 wt %) in the powder is so high that it might reflect full occupation of free nonmetallic lattice vacancies with oxygen atoms to form vanadium oxycarbide. In this connection, we analyzed in detail the state of oxygen in the sample. According to the data of quantitative gas chromatography, the main part of oxygen (3.1 wt %) is in the chemisorbed form. An additional 1.8 wt % is in the formed of adsorbed water (water content of 2 wt % was determined by calcination in a vacuum at 500 K and also by gas chromatography and thermogravimetry). A small amount of oxygen (0.1 wt %) is dissolved in the vanadium carbide lattice, occupying only a small fraction of carbon sublattice points (about 0.4%). Finally, a very small amount of oxygen forms the surface oxide layer consisting of 2–3 atomic monolayers. The film contains V_2O_3 and homologous oxides V_nO_{2n-1} whose composition lies between V_2O_3 and VO_2. The nitrogen content, determined without preliminary heating of the powder, is only 0.2 wt % and cannot noticeably affect the properties of the powder.

To analyze the oxide layer, we heated a carbide powder in dilute HCl (0.36 wt %, pH 1) at 330 K for several minutes. The light blue color of the resulting solution indicates that V(III) and/or V(IV) ions passed into the solution, confirming the presence of an oxide film on the surface of powder particles.

The microscopic examination of the vanadium carbide powder revealed the following. Separate irregular-shaped agglomerates of 5–50 μm size (Fig. 1), consisting of ~1-μm particles, are visible at a ~1000× magnification. However, it becomes evident at a larger magnification that these particles have a complex structure and actually consist of a large number of very fine nanometric particles (we will term them further nanoparticles or nanocrystallites). For example, it is evident at a 10000× magnification that each of the objects of ~1 μm size resembles an opened rosebud or a very loose head of cabbage and consists of nanocrystallites. Electron micrographs obtained at 20000× and 30000× magnifications on a Gemini DSM-982 high-resolution scanning electron microscope (Figs. 2 and 3,

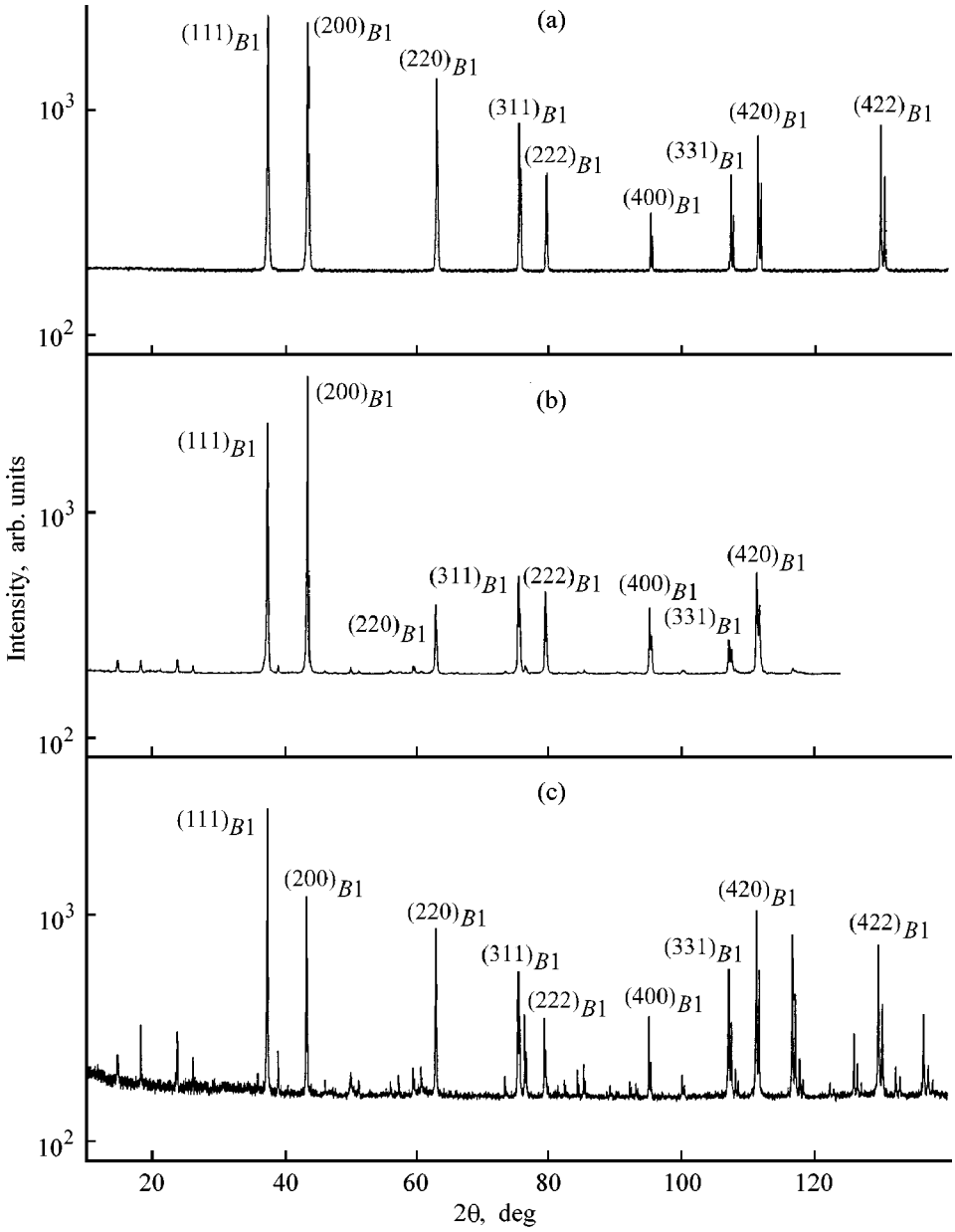

Fig. 4. X-ray diffraction patterns of powders of (a) disordered carbide $VC_{0.875}$, (b) ordered coarse-grained carbide $VC_{0.875}$ (V_8C_7), and (c) nanostructured carbide $VC_{0.875}$ ($CuK_{\alpha_{1,2}}$ radiation, intensity is plotted in a logarithmic scale, structural reflections of the *B*1 phase are marked). Superstructural reflections in Figs. 4b and 4c correspond to the cubic (space group $P4_332$) ordered V_8C_7 phase. High intensity I_{super} of superstructural reflections of $VC_{0.875}$ nanopowder and abnormal increase in I_{super} of the nanopowder in the region of $2\theta > 100°$ may be due to considerable static displacements of vanadium atoms.

respectively) show that nanocrystallites have a shape of leafs or lobes, which, when integrated, form a structure resembling corals. This nanostructure of vanadium carbide has no reported analogs. To a first approximation, nanocrystallites can be modeled by a disk with a diameter from 400 to 600 nm and a thickness of ~15–20 nm. Such a disk corresponds in volume to a relatively large spherical particle 150–220 nm in diameter, but, because of its small thickness, the ratio of its surface area *S* to volume *V* is $S/V = 0.107–0.143$ nm^{-1}, which corresponds to the specific surface area of the powder from 19 to 26 m^2 g^{-1}. The electron microscopy also shows that the size of nanocrystallites varies within a narow range.

The crystal structure was studied by X-ray diffraction in $CuK_{\alpha_{1,2}}$ radiation on a Siemens D-500 autodiffractometer in the mode of stepwise scanning with

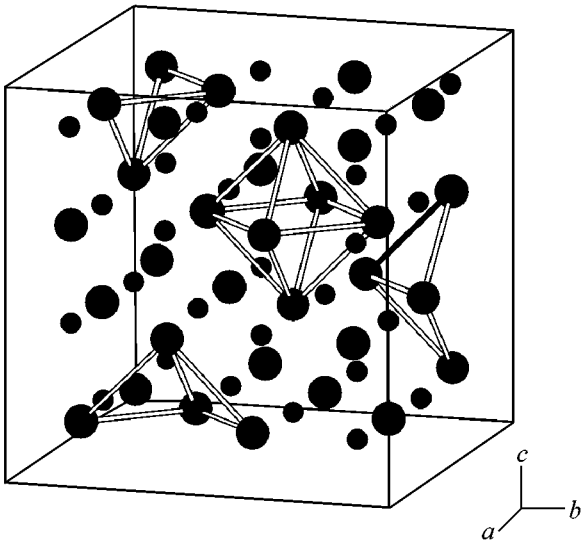

Fig. 5. Positions of vanadium (*large circles*) and carbon (*small circles*) atoms in a unit cell of ordered cubic (space group $P4_332$) phase of V_8C_7: vacant (not occupied by carbon atoms) octahedral interstices of the metallic sublattice are shown.

a step $\Delta 2\theta = 0.02°$ and accumulation time of 10 s in each point. The X-ray diffraction patterns of disordered carbide $VC_{0.875}$, annealed coarse-grained ordered carbide $VC_{0.875}$ (V_8C_7), and nanostructured carbide $VC_{0.875}$ are shown in Fig. 4. The X-ray pattern of the $VC_{0.875}$ nanopowder (Fig. 4c) contains only superstructural reflections corresponding to the cubic ordered V_8C_7 phase (space group $P4_332$) along with structural reflections of the *B*1 basic phase. The lattice spacing of the ordered phase is 0.8337 ± 0.0001 nm. An ideal cubic M_8C_7 superstructure corresponding to the $P4_332$ space group (Fig. 5) has a doubled (as compared to the disordered *B*1 basic phase) lattice spacing [7, 12]; therefore, the spacing of the basic phase of vanadium carbide under study is $a_{B1} = 0.41685$ nm. It is noticeably greater (by 0.00047 nm) than the spacing in the disordered carbide $VC_{0.875}$. According to [7, 8, 17], the difference in the spacings of ordered and disordered $VC_{0.875}$ carbides can be so large only at the maximal or close to maximal ordering.

The intensity ratio of structural and superstructural reflections confirms the fact that the degree of long-range ordering in vanadium carbide is close to a maximum. Furthermore, it follows from this ratio that the ordered phase occupies the whole volume of the substance, i.e., the powder is single-phase. This ratio also allows us to make an important conclusion that the content of oxygen in the carbide lattice is small, in agreement with the oxygen content as low as 0.1 wt % determined by chemical analysis.

It is interesting that the intensity of superstructural reflections I_{super} of the coarse-crystalline ordered carbide $VC_{0.875}$ decreases with increasing diffraction angle 2θ (Fig. 4b), whereas the intensity of superstructural reflections of the vanadium carbide nanopowder in the region $2\theta > 100°$ not only does not decrease, but even grows (Fig. 4c). This may be due to the presence of considerable relaxation static displacements of vanadium atoms in the vicinity of carbon vacancies. Earlier such displacements were detected in the ordered carbide V_8C_7 [16].

In spite of the nanometer thickness of nanocrystallites, we found no essential deviations of the width of diffraction reflections from the instrumental width. As all the atoms inside a crystallite scatter coherently, the lack of diffraction line broadening agrees with the presence of a fairly large number of atoms in nanocrystallites because of their large size in two dimensions.

We measured the density of vanadium carbide powder by the vacuum pycnometric method using purified kerosene (middle fraction) and distilled water as working liquids. The error in the determination of the pycnometric density did not exceed 0.5%. The calibration measurements of the pycnometric density of single-crystalline silicon have confirmed the reliability and accuracy of the measurements: the theoretical density of silicon is 2.330 g cm^{-3}, and the measured pycnometric density was 2.236 g cm^{-3}, i.e., the disagreement was less than 0.2%.

The pycnometric density of nanostructured $VC_{0.875}$ powder of 5.15 g cm^{-3} was much less than the theoretical density. A reason could be the presence of a low-density component (for example, physically adsorbed water) in the sample or high defectiveness of the metallic sublattice due to the presence of vacant points (vacant metal positions). To reveal the role of these factors, we have measured the pycnometric density after calcination of the carbide in a vacuum. After the removal of water at 470 K, the pycnometric density increased to 5.48 g cm^{-3}, which is also somewhat less than the theoretical density and is due to the presence of chemisorbed oxygen. Only after annealing at 900 K in a vacuum, the pycnometric density increased to 5.62 g cm^{-3}, which is equal to the theoretical value. The fact that the theoretical density was reached as a result of annealing at 900 K, when the diffusion of atoms in the metal sublattice is negligibly small, means that the metal sublattice contains no structural vacancies, and the reduced initial density was due to adsorbed impurities of water and oxygen. Though one or two atomic layers of oxides still re-

main on the surface of nanocrystallites after the annealing at 900 K, we failed to reveal a difference between the theoretical and pycnometric densities, as the content of the surface oxide phase is less than 0.1 wt %, and the densities of vanadium oxides and carbide are close.

Compact samples. We prepared samples of compact nonstoichiometric vanadium carbide $VC_{0.875}$ by hot pressing of a powder of disordered carbide $VC_{0.875}$ at 2000 K and a pressure of 20–25 MPa in a stream of ultrapure argon. The resulting samples were subjected to three kinds of heat treatment: annealing at 1370 K for 2 h followed by slow cooling (100 K h^{-1}) to 300 K and quenching from 1420 and 1500 to 300 K. The quenching mode was as follows: Samples in quartz ampules evacuated to 10^{-3} Pa were annealed at 1420 and 1500 K for 15 min and then quenched in water (100 K s^{-1}). An electron micrograph (500× magnification) of the surface of a compact $VC_{0.875}$ specimen after quenching from 1500 K is shown in Fig. 6. Since boundaries of basic phase grains show increased sensitivity to oxidation, they are clearly visible in the electron micrograph obtained on an ISI DS-130 scanning electron microscope. The grain size ranges from 10 to 60 μm.

The structure of annealed and quenched $VC_{0.875}$ samples was studied by X-ray diffraction. Along with structural reflections, the X-ray diffraction patterns contain weak additional reflections both after annealing and after quenching (Fig. 7). Our study has shown that the additional reflections are superstructural and correspond to the ordered cubic V_8C_7 phase (space group $P4_332$). The superstructural reflections for the annealed and quenched samples have approximately equal integral intensities but different width. The superstructural reflections in the X-ray pattern of the sample quenched from 1500 K are the broadest.

According to the equilibrium phase diagram of the V–C system [7, 8, 18], the ordered V_8C_7 phase is formed as a result of the disorder–order transition at T_{trans} = 1380 K; the experimental temperature of the phase transition is 1413 ± 20 K [14]. These data show that fast cooling from 1420 or 1500 K could result in quenching of the disordered nonstoichiometric vanadium carbide $VC_{0.875}$ and in its preservation as a metastable phase. However, the ordered V_8C_7 phase appears even on quenching from 1500 K, with the relative intensity of the superstructural reflections being approximately the same as for the sample quenched from 1420 K or annealed at 1370 K (Fig. 7).

As a result of ordering, each grain of the basic disordered phase is broken into domains of the ordered

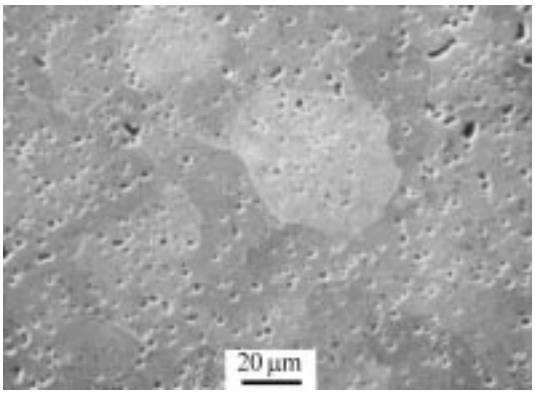

Fig. 6. Microstructure of the surface of compact $VC_{0.875}$ after quenching from 1500 K (500× magnification).

phase. The degree of ordering in a domain is high, and the mutual arrangement of the domains is as chaotic as allowed by the relationship between the structures of the ordered phase and disordered matrix. The width of structural reflections does not depend on the conditions of heat treatment of compact $VC_{0.875}$ samples, suggesting that the grain size of the basic phase does not change on ordering. However, the superstructural lines are noticeably broadened, which may be due to small size of domains of the ordered phase formed under various heat treatment conditions. The following questions arise: Is the nanostructure formed in heat-treated compact $VC_{0.875}$ samples containing the ordered V_8C_7 phase? How small are the domains of the ordered phase? To answer these questions, it is necessary to measure the width of the experimental diffraction reflections and to compare it to the diffractometer resolution function.

We determined the resolution function of a Siemens-D500 automatic diffractometer by a special diffraction experiment with an annealed sample of stoichiometric tungsten carbide with a grain size of 10–20 μm. Tungsten carbide has no homogeneity area; therefore, there is no line broadening due to inhomogeneity; the size broadening of diffraction lines is also absent with such grains. Owing to annealing of the sample, deformation broadening is also absent. Thus, the width of diffraction reflections of tungsten carbide practically coincides with the diffractometer resolution function for a given diffraction angle θ. The dependence of the second moment θ_R of the resolution function of a Siemens D-500 diffractometer on the diffraction angle θ is shown in Fig. 8. To describe analytically the diffraction reflections, we used a pseudo-Voigt function. We have shown that, in this case, the full width of a diffraction reflection at half-maximum (2Δ) is related to the second effective moment θ of the reflection under consideration by $2\Delta = 2.235\theta$.

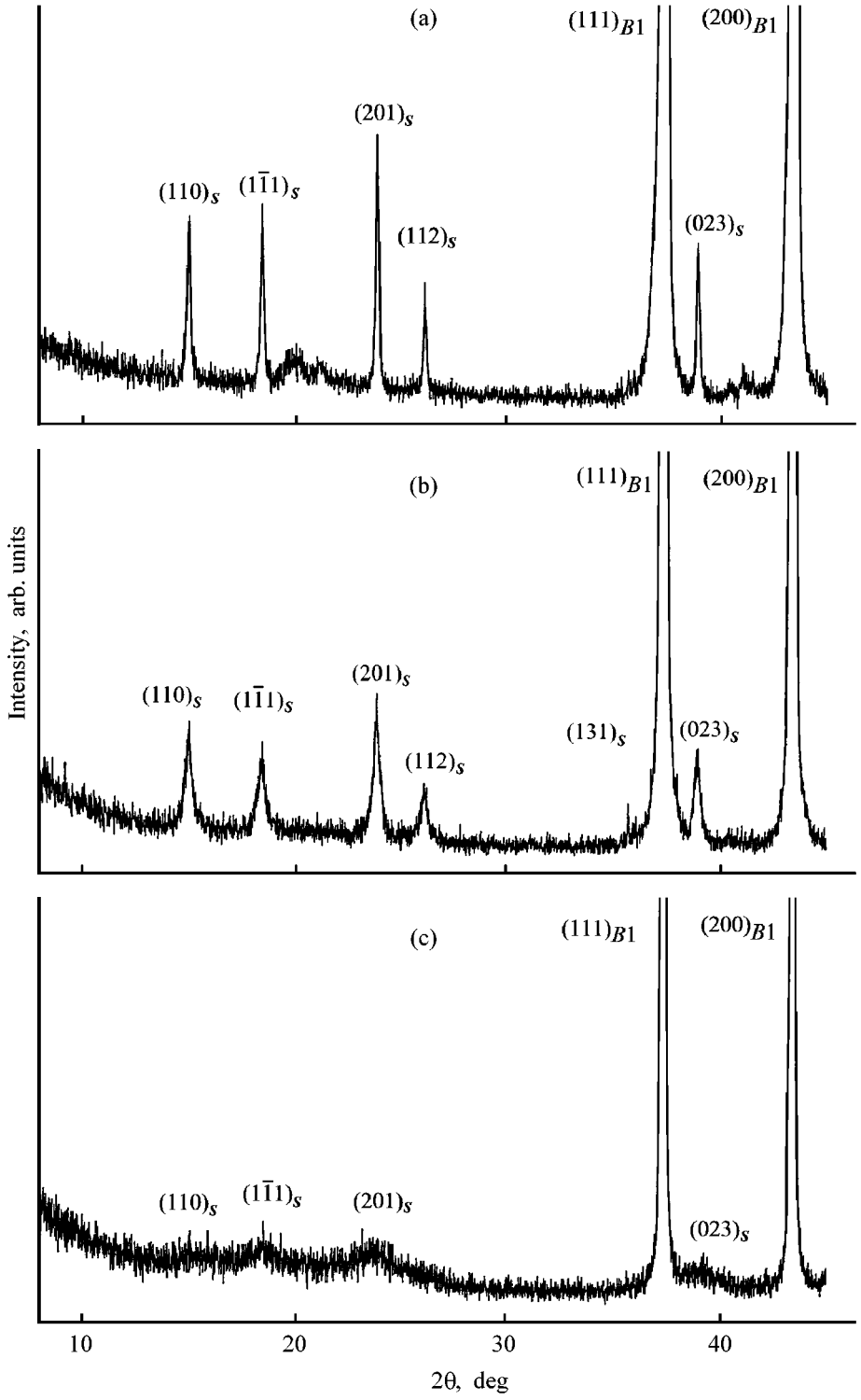

Fig. 7. X-ray patterns of compact $VC_{0.875}$ obtained by hot pressing, after heat treatment (Cu$K_{\alpha_{1,2}}$ radiation, structural reflections of the *B*1 phase and superstructural reflections of the V_8C_7 phase are marked). (a) Annealing at 1370 K for 2 h followed by slow cooling to 300 K; (b) quenching from 1420 to 300 K at a cooling rate of 100 K s^{-1}; amd (c) quenching from 1500 to 300 K at a cooling rate of 100 K s^{-1}. Superstructural reflections of the cubic (space group $P4_332$) ordered V_8C_7 phase are observed in all the patterns; the most broadened superstructural reflections are observed in the pattern of the $VC_{0.875}$ sample quenched from 1500 K.

The comparison of the width of superstructural diffraction reflections of a compact vanadium carbide sample with the diffractometer resolution function θ_R has shown that the experimental reflections are broadened (Fig. 8). As the width of these reflections depends on the domain size and resolution of an instrument in use, the measurement of the broadening β allows us to determine the size of domains. In view of the ratio $2\Delta = 2.235\theta$, the reflection broadening is

$$\beta = [(2\Delta_{exp})^2 - (2\Delta_R)^2]^{1/2} \equiv 2.235\ [\theta^2_{exp} - \theta^2_R]^{1/2}.$$

To a first approximation, let us assume that the deformation broadening is absent and the observed broadening β results only from small size of domains; thus, $\beta = \beta_s$. In turn, the size broadening measured in radians $\beta_s(2\theta) \equiv 2\beta_s(\theta)$ is related to the average domain size d by

$$d = \frac{k\lambda}{\beta_s(2\theta)\cos\theta} \equiv \frac{k\lambda}{2\beta_s(\theta)\cos\theta},$$

where $k \sim 1$ is the form factor of a particle (crystallite or domain) and λ is the radiation wavelength.

Figures 7 and 8 show that the superstructural reflections are the most broadened in the case of a sample quenched from 1500 K; the superstructural reflections of a vanadium carbide sample annealed at 1370 K are the least broadened. This means that the domains of the ordered phase are the smallest in the sample quenched from 1500 K. The domains are the largest in the annealed sample of vanadium carbide, as the annealing followed by slow cooling is more favorable for domain growth. The determination of the broadening β_s and subsequent estimation of the average size d of the ordered phase domains by the above-mentioned formula gave the following data. The domain size is 54 ± 5 nm (95% confidence level) in the annealed samples (Fig. 7a) and 25 ± 4 and 8 ± 5 nm in the samples quenched from 1420 (Fig. 7b) and 1500 K (Fig. 7c), respectively.

Thus, the annealing and quenching of compact samples of nonstoichiometric vanadium carbide $VC_{0.875}$ from $T_{trans} \pm 100$ K give rise to a nanostructure consisting of the ordered phase domains. The domain size is the greater, the lower the annealing (or quenching) temperature and the slower the cooling.

ELECTRON–POSITRON ANNIHILATION

Electron–positron annihilation is the most efficient and sensitive method for studying defects on interfaces and surfaces of nanoparticles. Capture of positrons by such defects as vacancies or nanopores results in prolonged lifetime of positrons as compared to that in defect-free materials [4]. The positron lifetime furnishes information on the defect type.

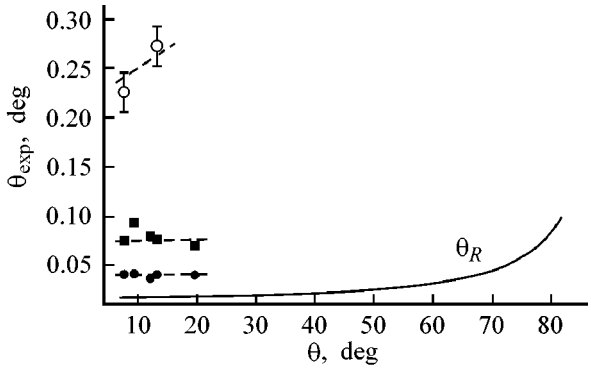

Fig. 8. Broadening of diffraction reflecions of compact $VC_{0.875}$ samples after heat treatment and appearance of the ordered V_8C_7 phase [comparison of the second moments θ_{exp} of diffraction reflections with the angular dependence of the second moment $\theta_R(\theta)$ $\{\theta_R = [(0.0052\tan^2\theta + 0.0056)^{1/2}]/[4(2\ln 2)^{1/2}]\}$ of the diffractometer resolution function]. *Dark circles*: annealing at 1370 K followed by slow cooling; *dark squares*: quenching from 1420 K; and *light circles*: quenching from 1500 K. The angular dependence of the diffractometer resolution function $\theta_R(\theta)$ is shown by a *solid line*.

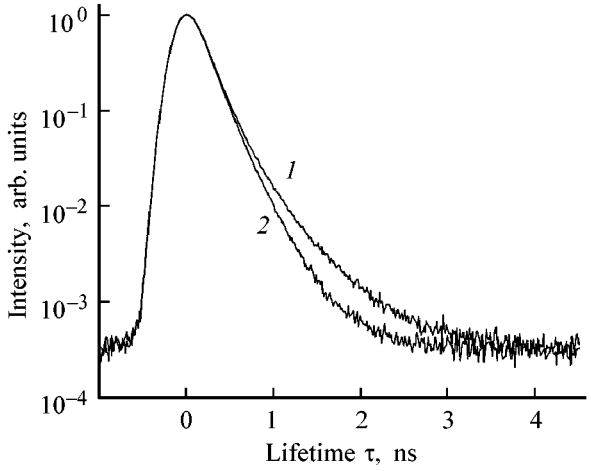

Fig. 9. Lifetime spectra of positrons of nanostructured powder of (*1*) vanadium carbide $VC_{0.875}$ and (*2*) coarse-grained vanadium carbide $VC_{0.875}$.

We measured the lifetime of positrons using a $VC_{0.875}$ powder preliminarily calcined at 400 K to remove water. For comparison, we measured the positron lifetime in a coarse-crystalline sintered sample of vanadium carbide of the same composition $VC_{0.875}$. The positron lifetime spectra are shown in Fig. 9. It is seen from the spectra that the average lifetime of positrons in the nanopowder appreciably exceeds that

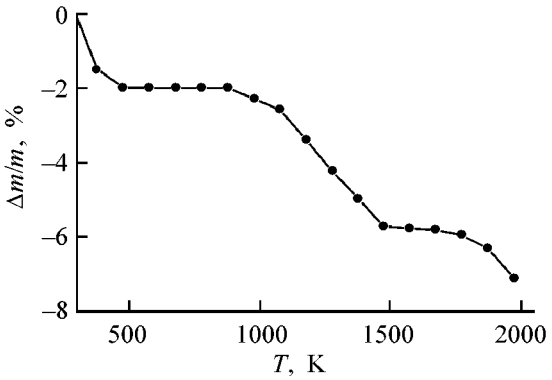

Fig. 10. Relative weight change $\Delta m/m$ of a $VC_{0.875}$ sample on stepwise sintering in a vacuum.

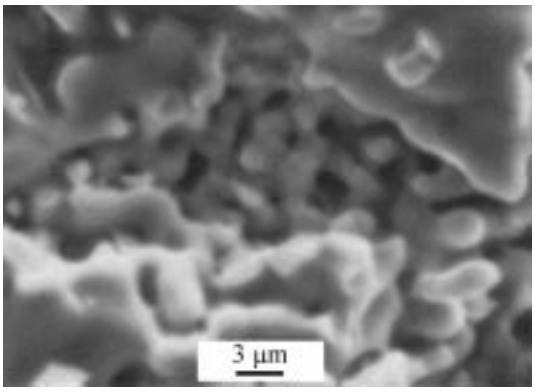

Fig. 11. Microstructure of sintered nanopowder of vanadium carbide, determined with a scanning electron microscope. Both very densely sintered agglomerates and a free space between them up to 10 μm in size are seen.

in a polycrystal. The spectrum of the coarse-crystalline sample of vanadium carbide exhibits only a short component, 157 ± 2 ps, which corresponds to the annihilation of positrons in structural vacancies of the carbon sublattice [19, 20]. Quantitative analysis of the spectrum of the powdered sample has shown that, along with a short-life component at 157 ± 2 ps, it contains a long-life component at 500 ps with the relative intensity I_2 = 7%. According to [4], the long-life component corresponds to the annihilation of positrons in surface defects of particles. The capture of positrons by a structural vacancy means the absence of the long-distance positron diffusion; in this case, the component intensities are proportional to the volume fractions of the phases containing various defects. Thus, the relative intensity of the long-life component I_2 coincides with the volume fraction of the surface $\Delta V_{surf} = \Delta DS/V$ in the vanadium carbide nanopowder. We estimated that the surface layer has the thickness ΔD = 0.5–0.7 nm, which corresponds to 3–4 atomic monolayers.

Thus, the measurements of the positron lifetime have shown that the internal part of nanocrystallites of dispersed vanadium carbide contains only nonmetallic structural vacancies, whereas in the surface layer of nanocrystallites there are defects like vacancy agglomerates.

SINTERING AND MICROHARDNESS

The $VC_{0.875}$ powder was cold-pressed at 10 MPa. The density of the pressed sample was 68% of the theoretical density of vanadium carbide, which is much higher than the bulk density of the powder (36%). The stepwise sintering of a pellet was carried out in a vacuum (10^{-3} Pa) at temperatures from 400 to 2000 K in 100 K steps, for 2 h at each temperature. We found no noticeable changes in the density of the sintered sample as compared to that of the pressed sample.

The relative weight loss $\Delta m/m$ of a sintered sample with temperature is shown in Fig. 10. Three main stages of the weight loss can be distinguished. The first stage, from room temperature to 500 K, involves the water loss on calcination. The second stage, 900–1500 K, involves decomposition and removal (owing to the presence of a small amount of free carbon in the sample) of the surface oxide phase. After sintering in this temperature range, the sample has changed the color from black, caused by the surface oxide phase, to characteristic gray, corresponding to pure vanadium carbide. The third stage of weight loss, starting at 1900 K, is due to congruent vacuum evaporation of vanadium carbide $VC_{0.875}$ [9].

In spite of considerable porosity (about 30%) of the sintered sample, it appeared possible to measure its Vickers microhardness. The measurements were carried out in the automated mode with loads of 200 and 500 g and loading time of 10 s. Within the limits of experimental accuracy, we have revealed no dependence of the microhardness on the load. The microhardness H_V was 60–80 GPa. For comparison, we have measured the microhardness of a sample of coarse-grained $VC_{0.875}$ obtained by hot pressing; it was 21 GPa under a load of 0.1 kg. According to the published data [21], the microhardness of coarse-grained vanadium carbide is 29 GPa under loads of 0.1 and 0.2 kg. Thus, the microhardness of a sample obtained by sintering vanadium carbide nanopowder exceeds 2–3 times that of coarse-grained vanadium carbide and approaches the microhardness of diamond. In fact, at 300 K the microhardness of nanomaterials is 2–7 times higher than that of a usual polycrystalline material [1, 2]. The much higher microhardness of $VC_{0.875}$ obtained by sintering a nano-

powder is attributable to the Hall–Patch law, according to which H_V is proportional to $d^{-1/2}$. An examination [3] of experimental data on the microhardness of compact nanocrystalline materials has shown that the Hall–Patch law is obeyed within the range of grain size d from 500 to 20 nm. The dispersed carbide of which the sample was sintered corresponds to this range of the nanocrystallite size.

At the same time, it should be noted that we failed to detect a nanostructure in the sintered $VC_{0.875}$ sample. Examination of the sample on an ISI DS-130 scanning electron microscope has shown that its microstructure contains very well sintered agglomerates and a free space between them (Fig. 11). This observation is in good agreement with high porosity of the sample. To find whether the sintered agglomerates have a nanostructure, additional studies are required using high-resolution transmission electron microscopy.

No superstructural reflections were revealed in the X-ray diffraction patterns of the sintered sample. It is understandable, as the maximal sintering temperature (2000 K) is much higher than the temperature T_{trans} of the order–disorder phase transition. To reach the ordered state in the sample, the heat treatment should be performed at a temperature close to T_{trans}.

To conclude: The formation of a nanostructure of dispersed and compact nonstoichiometric vanadium carbide $VC_{0.875}$ is due to the disorder–order phase transition $VC_{0.875} \rightarrow V_8C_7$ in this carbide. Nanocrystallites of dispersed ordered nonstoichiometric vanadium carbide have the shape of strongly bent plates (disks) from 400 to 600 nm in diameter and 15–20 nm thick. The internal part of a nanocrystallite consists of ordered V_8C_7 with a high degree of long-range order and negligibly low content of dissolved oxygen. Chemisorbed oxygen in amount of 3.1 wt % and a considerable number of vacancy agglomerates are present in the surface layer of nanocrystallites, indicating their loose structure. The thickness of the surface phase does not exceed 0.7 nm or four atomic monolayers.

The observed morphology of nanocrystalline powder of nonstoichiometric vanadium carbide may originate from grain cracking on interfaces between the disordered and ordered phases. In fact, high-temperature X-ray measurements [14] showed that, at 1413 ± 20 K, the lattice spacing of the crystalline face-centered cubic sublattice increases jumpwise by 0.4 pm as a result of the disorder–order phase transition $VC_{0.875} \rightarrow V_8C_7$; the size of domains of the ordered phase is ~20 nm. According to [15, 17], the ordering $VC_{0.875} \rightarrow V_8C_7$ takes place at 1368 ± 12 K by the mechanism of the first-kind phase transition. At 300 K, the parameter a_{B1} of the basic crystal lattice of quenched disordered carbide $VC_{0.87}$ is less by 0.2 pm than that of the ordered carbide with the same carbon content [15, 17]. The difference in volumes between the disordered and ordered phases gives rise to stresses and subsequent cracking along phase boundaries. The cracking of grains of the initial disordered phase can occur also along boundaries of antiphase domains of the ordered phase owing to mismatch of their atomic structures and arising stresses.

In compact samples of nonstoichiometric vanadium carbide $VC_{0.875}$, another mechanism of the nanostructure formation is operative. A disorder–order transition results in the formation of ordered phase domains. The higher the temperature from which a heat treatment (quenching or annealing) is carried out, and the higher the cooling rate, the smaller are the domains.

On the whole, our study shows that ordering is an effective tool for creating nanostructures in dispersed and compact nonstoichiometric compounds. Presumably, the disorder–order transitions occurring with volume change can be used to generate nanostructural states of other materials, including strongly nonstoichiometric compounds.

ACKNOWLEDGMENTS

The authors are grateful to H. Labicka and A. Weisshart for taking electron micrographs of vanadium carbide and to O.V. Makarova for assistance in certification of vanadium carbide.

This work was financially supported by the Russian Foundation for Basic Research (project no. 99-03-32208a).

REFERENCES

1. Gusev, A.I., *Nanokristallicheskie materialy: metody polucheniya i svoistva* (Nanocrystalline Materials: Preparation Methods and Properties), Yekaterinburg: Ural. Otd. Ross. Akad. Nauk, 1998.
2. Gusev, A.I. and Rempel', A.A., *Nanokristallicheskie materialy* (Nanocrystalline Materials), Moscow: Fizmatlit, 2000.
3. Gusev, A.I., *Usp. Fiz. Nauk*, 1998, vol. 168, no. 1, p. 55.
4. Würschum, R. and Schaefer, H.-E., *Nanomaterials: Synthesis, Properties, and Applications*, Edelstein, A.S. and Cammarata, R.C., Eds., Bristol: Inst. of Physics, 1996, p. 277.
5. Gleiter, H., *Nanostruct. Mater.*, 1995, vol. 6, nos. 1–4, p. 3.

6. *Svoistva, poluchenie i primenenie tugoplavkikh soedinenii: Spravochnik* (Properties, Preparation, and Application of Refractory Compounds: Handbook), Kosolapova, T.Ya., Ed., Moscow: Metallurgiya, 1986.
7. Gusev, A.I., Rempel, A.A., and Magerl, A.J., *Disorder and Order in Strongly Nonstoichiometric Compounds: Transition Metal Carbides, Nitrides, and Oxides*, Berlin, 2001.
8. Gusev, A.I. and Rempel', A.A., *Nestekhiometriya, besporyadok i poryadok v tverdom tele* (Nonstoichiometry, Disorder, and Order in Solids), Yekaterinburg: Ural. Otd. Ross. Akad. Nauk, 2001.
9. Gusev, A.I., *Fizicheskaya khimiya nestekhiometricheskikh tugoplavkikh soedinenii* (Physical Chemistry of Nonstoichiometric Refractory Compounds), Moscow: Nauka, 1991.
10. Gusev, A.I. and Rempel', A.A., *Strukturnye fazovye perekhody v nestekhiometricheskikh soedineniyakh* (Structural Phase Transitions in Nonstoichiometric Compounds), Moscow: Nauka, 1988.
11. Rempel', A.A., *Effekty uporyadocheniya v nestekhiometricheskikh soedineniyakh vnedreniya* (Ordering Effects in Nonstoichiometric Intercalation Compounds), Yekaterinburg: Nauka, 1992.
12. Rempel', A.A., *Usp. Fiz. Nauk*, 1996, vol. 166, no. 1, p. 33.
13. Gusev, A.I. and Rempel, A.A., *Phys. Status Solidi (A)*, 1993, vol. 135, no. 1, p. 15.
14. Athanassiadis, T., Lorenzelli, N., and Novion, C.H. de, *Ann. Chim.*, 1987, vol. 12, no. 2, p. 129.
15. Lipatnikov, V.N., Lengauer, W., Ettmayer, P., Keil, E., Groboth, G., and Kny, E., *J. Alloys Comp.*, 1997, vol. 261, p. 192.
16. Rafaja, D., Lengauer, W., Ettmayer, P., and Lipatnikov, V.N., *J. Alloys Comp.*, 1998, vol. 269, p. 60.
17. Lipatnikov, V.N., Gusev, A.I., Ettmayer, P., and Lengauer, W., *J. Phys.: Condens. Matter*, 1999, vol. 11, no. 1, p. 163.
18. Gusev, A.I., *Zh. Fiz. Khim.*, 2000, vol. 74, no. 4, p. 600.
19. Rempel', A.A., Foster, M., and Schaefer, H.-E., *Dokl. Ross. Akad. Nauk*, 1992, vol. 326, no. 1, p. 92.
20. Rempel, A.A., Zueva, L.V., Lipatnikov, V.N., and Schaefer, H.-E., *Phys. Status Solidi (A)*, 1998, vol. 169, no. 2, p. R9.
21. Ramqvist, L., *Jernkont. Ann.*, 1968, vol. 152, no. 9, p. 467.